Topoenergetic aspects of amorphous-crystalline coupling. I.Composite behaviour of water and aqueous solutions.*

Gh. Dragan, GDF – DATA BANKS, str.Abrud 25, Bucharest 78186, ROMANIA

1.Introduction

Intensive studies on structural modifications in polyethylenes (PE) as a result of applied thermal, mechanical and/or chemical treatments have revealed different participation of amorphous and crystalline phases [1-14]. Amorphous phase has a spectrum of configurational, spatial and dimensional distribution in a tested specimen as depending on its initial nature and the applied treatments. In general, any kind of PE has two distinct amorphous phases, namely one major as a continuous phase in which crystalline domains are dispersed containing conformational and configurational defects of the second amorphous phase .By a chemical treatment, for instance chlorination activated by UV radiation in aqueous suspension [2], these defects are grafted in two distinct stages corresponding to the two amorphous phases: the former mentioned one reacts first , faster and has great amplitude, while the second one reacts slowly with smaller amplitude. Dimensional and structural spectra of both amorphous phases depend on the initial nature of PE, so a species of high density PE has smaller continuous amorphous phase and greater crystalline domains than one species of low density PE.

Calorimetric measuring systems give information about both amorphous and crystalline phases, so in these morphological studies calorimetry has been proved as a highly efficient analytical tool by rapidity, simplicity, repeatability, sensitivity [2-8]. Differential thermal analysis (DTA) and its calibrated version - differential scanning calorimetry (DSC), were measuring systems basically used to evidence these structural modifications.

Figure 1 reproduces typical melting endotherms corresponding to a HDPE before and after successive chlorination an annealing. Melting of crystalline phase appears as an order-disorder process centered on a melting point Tmo. After chlorination the crystalline phase is specifically diminished by defect grafting and by their coherently precipitation in local amorphous domains (LAD) during annealing. Finally, a new ordered structure is formed in the crystalline domains (Figure 2, [9,10]) detected as a distinct melting process Tm1. Peak heights of Tmo and Tm1

* Work presented as poster at N&N 2000 (see EVENTS) and at N&N2001.

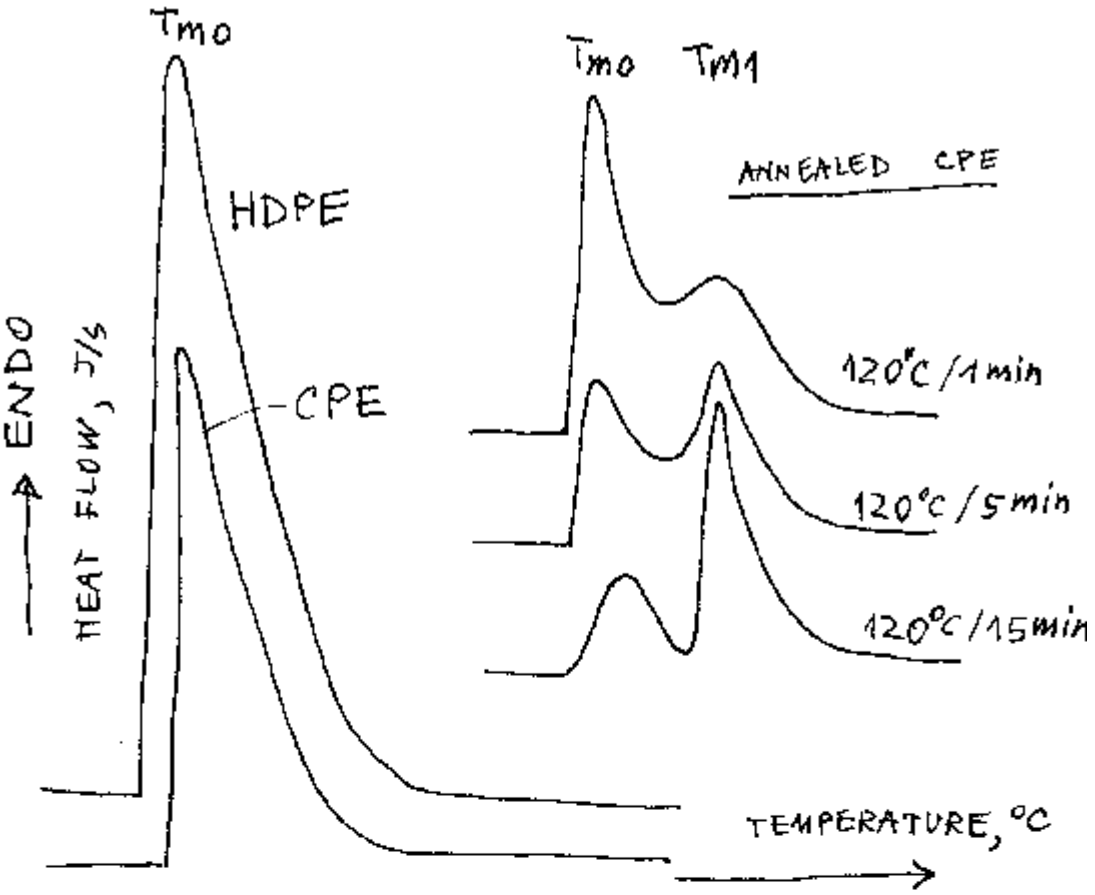

Figure 1. DTA melting endotherms of HDPE, CPE and annealed CPE specimens.

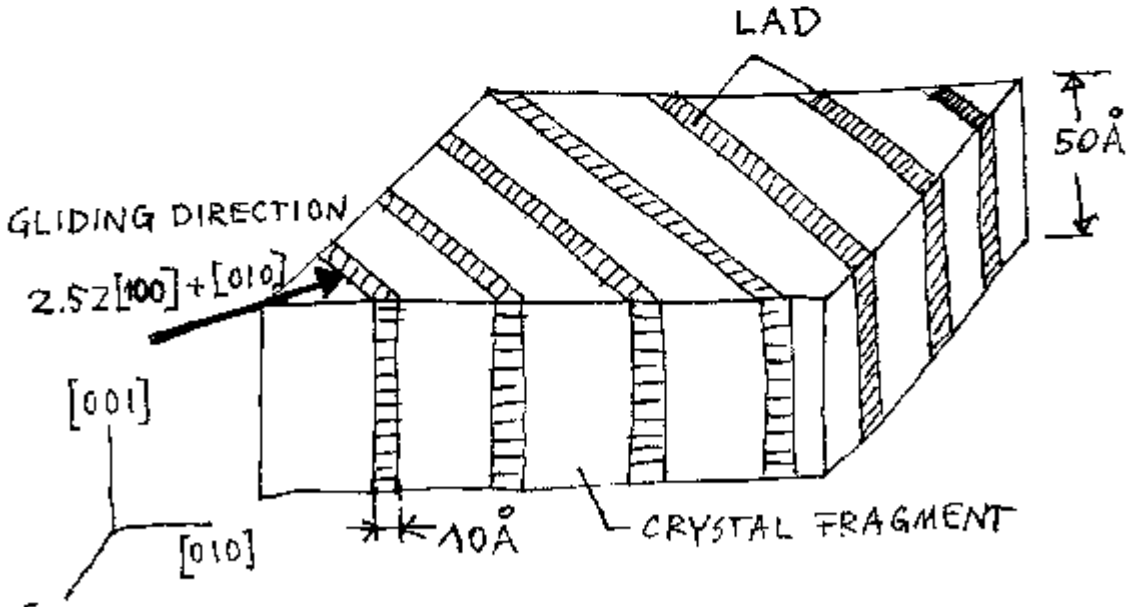

Figure 2. Morphology of a crystalline domain after coherent precipitation of chemically etched defects by annealing.

endotherms denoted as ho and h1 respectively, quantitatively express the crystalline phase of all crystalline fragments and the coupling strength between them and LAD. This coupling is much more stronger in this case than the coupling between continuous amorphous phase and crystalline domains. There are some cases, for instance cold drawn PE foils and yarns [11,12], for which Tm1 process represents the coupling between the continuous amorphous phase and the crystalline domains. Due the fact that the two processes in Figures 1 are in direct relationship, i.e. Tmo decreases while Tm1 increases, amorphous crystalline coupling (ACC) can be estimated by the splitting coefficient $\alpha = h1/(ho+h1)$. The energy stored in this ACC ranges between 10-50 J/g and can be measured by melting with high accuracy with a simple DTA device. This measuring system (MS) was called as *in vitro* MS because it evidences the effects of defect precipitation. It is possible to directly measure this process by an *in vivo* calorimetric MS, namely by transferring a calorimetric cell with CPE specimen from room temperature in an isothermal differential Calvet calorimeter at annealing temperature (called as drop calorimetry) [13,14]. Although the sensitivity of the calorimeter used was enough high to evidence the process amplitude, thermograms (represented by a single endotherm) did not show it for all tested CPE specimens and no difference between the first and second thermograms for the same sample it was observed. This fact appeared to be as unexplained by classical thermodynamics and implied a careful structural study of the phenomenon. Finally, the coexistence of two simultaneous processes with the same amplitude and opposite energy was supposed [1,14]. The origin of the second process was supposed by the fact that defect kinetic momentum changes its vector direction ($\mathbf{v}$) by precipitation in LAD and this creates an inductive element $L \sim |d\mathbf{v}/dt|$ which is able to annihilate the direct process originated from kinetic energy $\sim |v|^2$. This way, an energy circuit of the transforming specimen has been proposed by considering the existence of two main components, namely one as inert component responsible for the immediate endotherm observed by CPE annealing in drop calorimeter, and the transforming component responsible for the Tm1 process revealed by *in vitro* DTA. The two components are coupled by the inductive element L.

The next step after these findings was to check if an inductive effect exists by simultaneous annealing of two CPE specimens [14]. Figure 3 shows the top view of the brass block used for single annealing (as reference) and simultaneous annealing of two CPE specimens (in mixture with silicon oil) with cylindrical symmetry, but having different orientations in respect to the gravitational field. CPE paste was directly placed in orifices in brass block or in Pyrex tubes in view to compare the

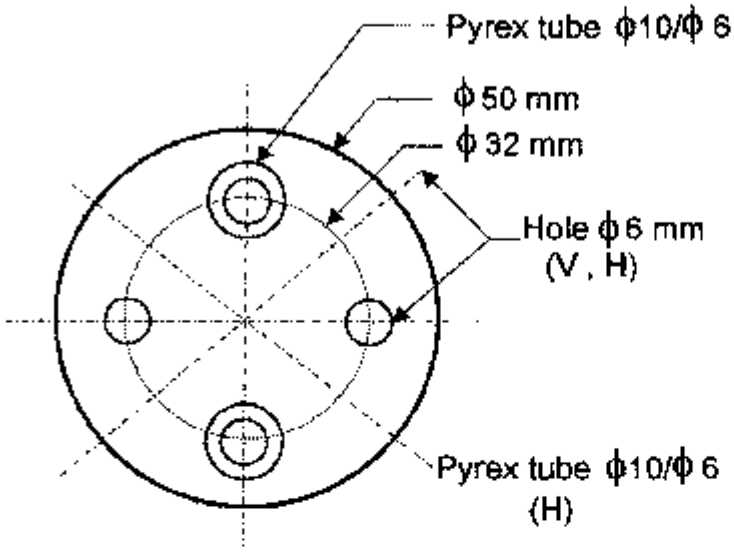

Figure 3. Top view of the brass block with the orifices for CPE specimens under annealing at 131.3 ± 0.1oC and subsequently tested by DTA.

V : vertical ; H : horizontal - relative to earth's gravity force field.

Block's height = 32 mm.

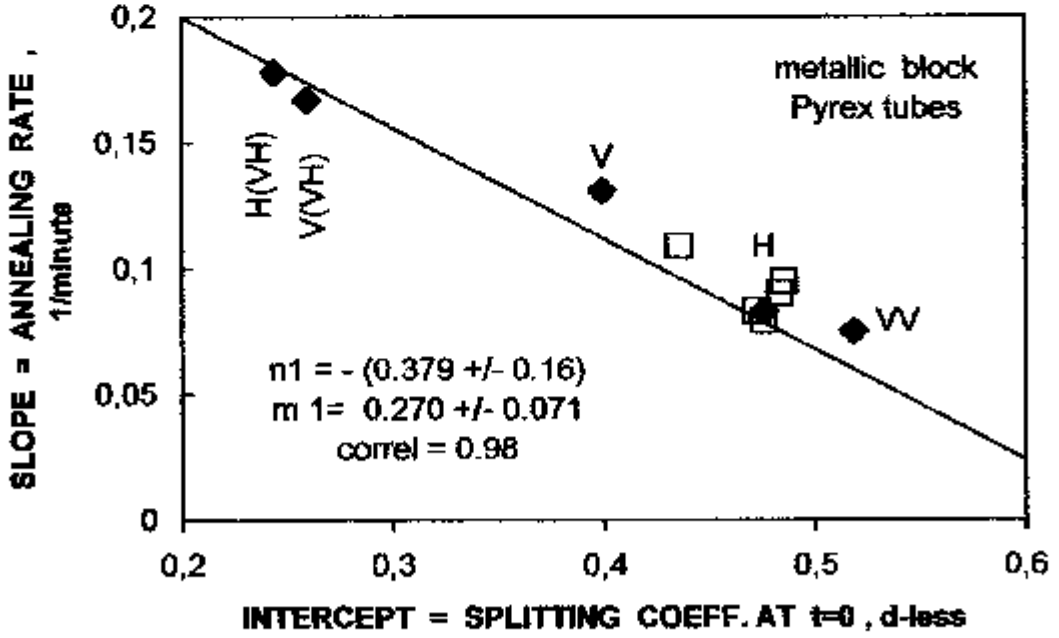

Figure 5. Affine representation of kinetic parameters for annealing process of CPE samples in different associations and orientations in respect to the gravitational field.

influence of dissipative coupling of the specimen to annealing temperature as driving potential. Structural differences are evidenced by the splitting coefficient α (as *in vitro* MS) averaged on at least 4 independent DTA measurements for the same annealed sample (the cylindrical annealed sample was cut in 4 - DTA specimens).Two main series of results were obtained corresponding to annealing in metallic block and in Pyrex tubes, respectively , and for each one three other series of results were distinct , namely :

V , H : vertical and horizontal annealing of single specimens
VV : simultaneous annealing of two vertical specimens
VH : simultaneous annealing of vertical and horizontal specimens.

Figure 4 shows these results for 3 annealing times in semilogarithmic scale, so a linear dependence is evident in all cases. Although net differences appear among the compared specimens, these can be better evidenced by slope and intercept parameters of these linear dependences as determined by linear regressions (Table 1). Figure 5 shows the affine relationship between these kinetic parameters which evidence the following important aspects of inductive coupling: (i) the experiments have been carried out in identical conditions for all compared specimens; (ii) the nature of the process evidenced by α is the same for all tested specimens; (iii) there are net differences in process amplitude between the three series of specimens annealed in metallic block, namely the rate of defect precipitation increases as it follows :

$$VV < H < V < H(VH) , V(VH) \qquad (1).$$

The existence of inductive element was also considered in other transforming systems [15]. Neutrino “particle” was firstly discovered also by calorimetry [16,17] and represents an inductive effect in β-decay processes.

These studies on a large variety of PE samples, were subsequently extended over other kinds of materials. Water and aqueous solutions represented a special case for which the solution process, their composite structure and the distribution of solute in solutions were the main aspects experimentally studied [18-23]. The same splitting process was evidenced by melting and freezing of water and aqueous solutions. The present study takes into account some simple facts evidencing new qualitative and quantitative aspects of ACC in water and aqueous solutions.

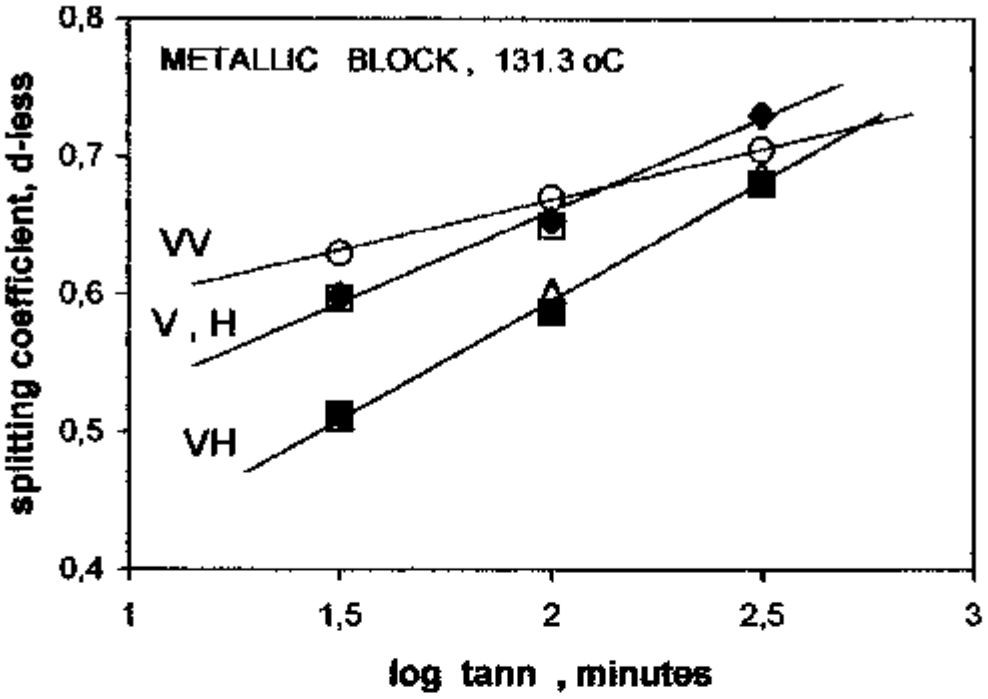

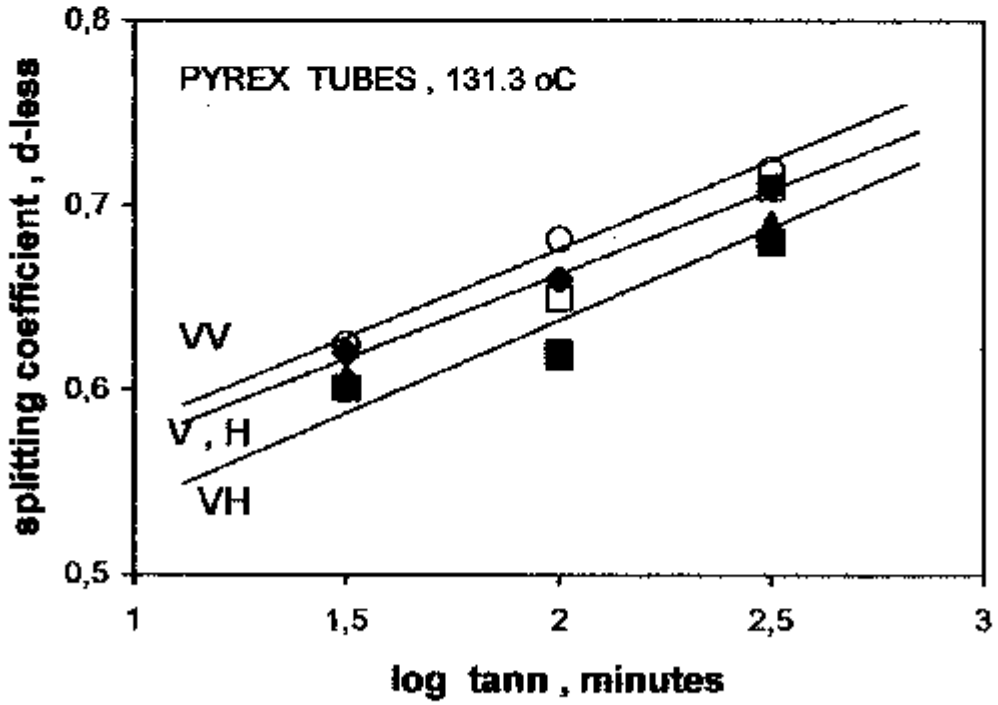

Figure 4. Annealing kinetics of separate and simultaneous CPE samples as developed by DTA in vitro MS [14].

2.Topoenergetic principles

Experiments on specimen behaviour as a function of different treatments and used MS, were allowed to reveal some general working principles in driving the experiments, retrieval of experimental data and in establishing the physical significances of the results.

One of the basic principle consists in considering that any transforming process has composite structure, i.e. it contains at least two components: one as inert, Cin and another one in transformation, Ctr. For instance Figure 6 shows the thermogram obtained by drop calorimetry [13] by transferring a specimen of liquid from T1>To (To= freezing point) in the calorimeter at T<To. This thermogram consists by two exotherms: the first one evolved immediately at the contact of the specimen with calorimeter , win and the second one ,wtr, which is delayed at a period of time , tin depending on T. The two heat flows correspond to the two main components separated by the freezing process of the liquid specimen, namely: Cin – the amorphous phase which does not participate to this process and Ctr – the crystalline phase responsible for freezing (crystallization) process, respectively.

By keeping the same measuring system and the operating procedure for a large variety of samples, the problem is to identify by comparison of their behaviours the nature and the amplitude of specific processes. In view to solve these problems, it is possible to consider the tested specimen as an energy circuit composed by components with elementary behaviour like in electric circuits. For instance the two components Cin and Ctr have capacitive behaviour and are coupled between them with dissipative and inductive elements. This idea was firstly introduced by Oster and Auslander [24] as topological representation of nonequilibrium systems, but considering the spatial distribution of an elementary circuit, so hard mathematical difficulties were arisen and they abandoned their attempt.

According to topoenergetic theory, the behaviour of a sample has meaning only in respect to a well-defined measuring system and standard operating procedure (SOP) concerning standard experimental conditions in obtaining the basic experimental data and the procedure to retrieve them [3]. The energy circuit does not depend directly by spatial coordinates, but the flows and potentials parameters depend only on time [8,13,25].In this way, Cin is located in laboratory reference frame, while Ctr has a different time reference frame. For thermally driven processes and considering the coupling between the two frames as purely dissipative, the following kinetic equation was established in Arrhenius representation [13]:

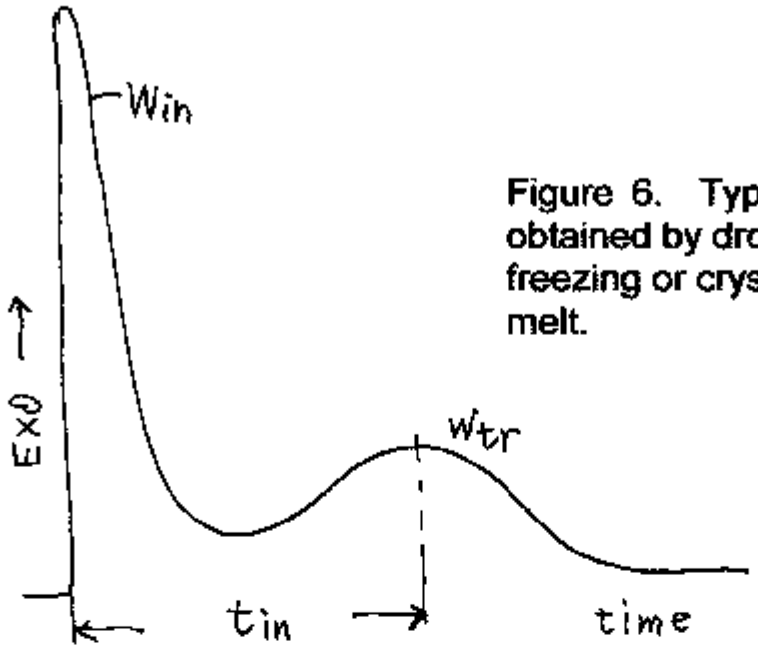

Figure 6. Typical thermogram obtained by drop calorimetry for freezing or crystallization from melt.

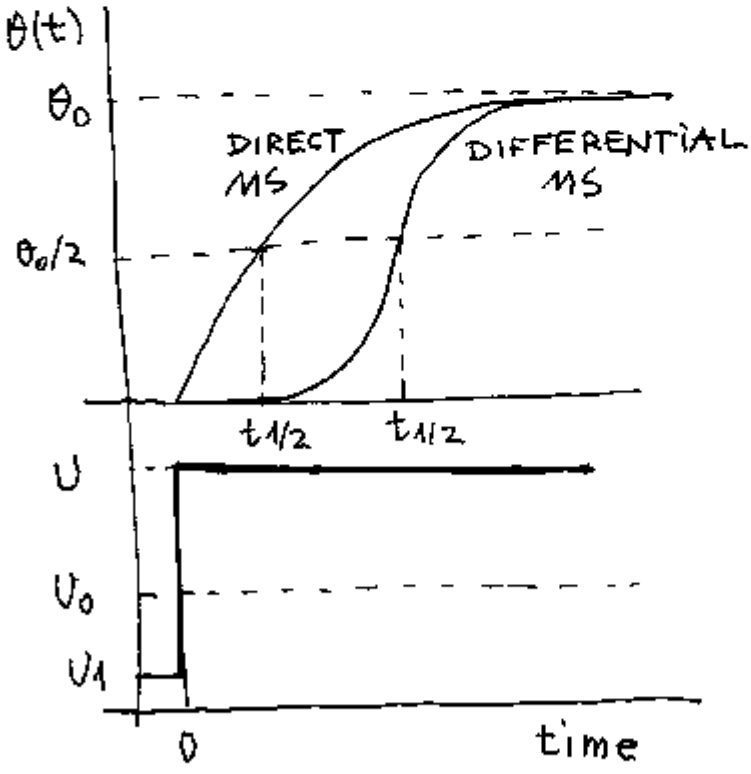

Figure 7. Typical conversions of a response function θ(t) as triggered by a stepwise perturbation of driving potential U passing through a threeshold value Uo.

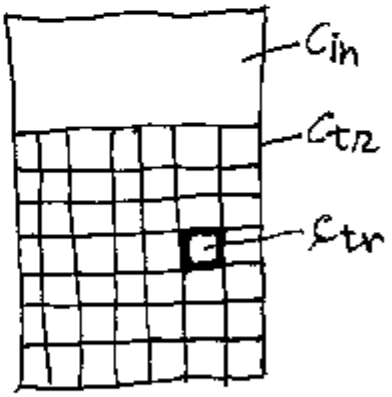

Figure 8. Schematically drawn of a standard specimen normalized in volume and shape.

$$\ln(tin*T) = -E/(RT) + K \quad (1),$$

where E – the activation energy and R- Boltzmann's gas constant.
It is important to notice that (tin,T) are the basic experimental data obtained by imposing to the tested specimens stepwise perturbation in temperature (for instance by drop calorimetry, Figure 6). If this SOP is correctly applied for a series of samples defining the same nature of the transforming process, the kinetic parameters (E, K) obey an affine relationship similar to that previously discussed (Figure 5), namely:

$$E = n1*K + m1 \quad (2),$$

where (n1,m1) parameters define the nature of the common process for the tested samples relative to the used SOP, so these are also called as the ***first phylogenic*** parameters. In fact, E or K define the amplitude of a particular sample or its ***ontogeny*** in the series because

$$K = \ln (Cin*R*E/R) \quad (3)$$

where *R* is the dissipative coupling constant between Cin and Ctr [13,26]. Another important aspect is that the algebraic sign of n1 systematically depends on the relative directions of the flows win and wtr. For instance, for crystallization from melt as it was considered previously, the two heat flows are exothermals and $n1 < 0$, while for polymerization [27] and thermal oxidation of amorphous phase in PE [28] win is endothermal and wtr is exothermal, so $n1 > 0$. These two distinct situations define the process ***polarity*** [29] , i.e. the increasing direction of process amplitude according to E or K parameters (see the cited particular examples).
It is important to remind that any kind of transforming process is triggered by transferring the tested specimen according to a specific SOP from an initial potential value U1 where it is in equilibrium, to a final one U through a threshold value Uo; this variation may be increasing or decreasing. The new equilibrium state at U can be experimentally observed by a ***response function***, $\theta(t)$, which in general has one of the dependence shape of time conversion as it is shown in Figure 7 and defining the direct or differential MS. Their pattern is defined by one characteristic parameter denoted as ***eigenvalue***, θ, which in practice is chosen as the half time of conversion, the saturation time, the saturation value , etc. The universal kinetic equation becomes as:

$$\ln \theta = N*\ln |U - Uo| + M \quad (4)$$

where (N,M,Uo) represent the ***ontogenic (kinetic) parameters***. For a series of samples tested according to the same SOP and have the same process nature, the following first phylogenic relationship exists:

$$N = n1*M + m1 \qquad (5).$$

It is also important to notice that all SOP in topoenergetic representations consider that tested specimens of a sample are identical and all specimens of all samples in series under comparison are normalized at the same shape and volume, so it is possible to schematically represent the structure specimen as in Figure 8.The process polarity (P) may be related to the process amplitude (Ctr), kinetic entity (ctr) and the coupling strength between Cin and Ctr (CS) as in the following Table :

Table 1.Relationship between process polarity and kinetic (ontogenic) parameters in Arrhenius and universal representations for $\theta \sim Ctr$.

sign(win*wtr)	P	sign(n1*E)	sign(n1*N)	M	-M/N	N^2/M
+	+	+	-	-lnCtr	-lnctr	CS
-	-	-	+	+lnCtr	+lnctr	

The units of Ctr, ctr and CS are relative to the considered SOP. Concerning to the process nature of a series of samples defined by (n1,m1), it is possible to consider one or many samples in this series as standard. In this way, data banks in topoenergetic meaning represent reference values of (N,M,Uo) , (n1,m1) and parameters of higher phylogenies for reference samples tested in specific SOP [30,31].

3.Solubility behaviour

Solubility represents one of the simplest and most important transforming process which can be treated on topoenergetic principles. It is basically driven by temperature, pressure and composition of one or both interacting components.

The composite structure of water and aqueous solution was evidenced by simple experiments [18-23]. Figure 9 reproduces in Arrhenius representation solubility behaviour of some hydrated ionic salts in water by considering θ= salt concentration at saturation in gram of anhydrous salt/gram of water [31,32]. At first sight it should be no difference between different hydrated forms of the same ionic salt, but there are important differences between their solubility behaviour because the

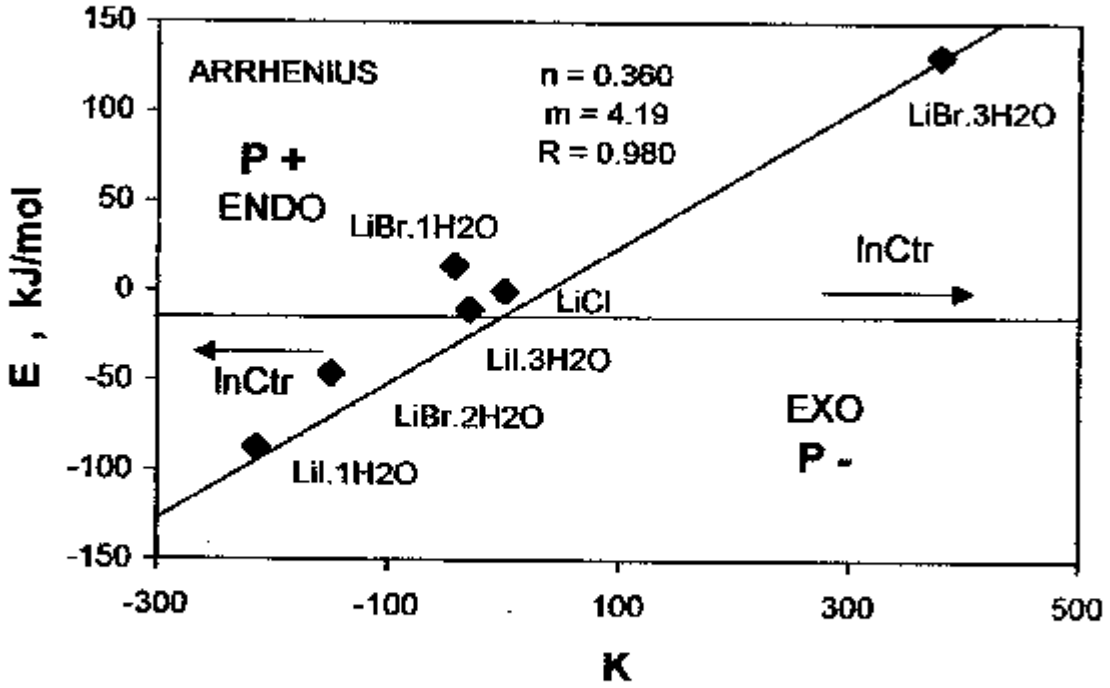

Figure 9. First philogeny in Arrhenius representation for solubility behaviour of several hydrated ionic salts.

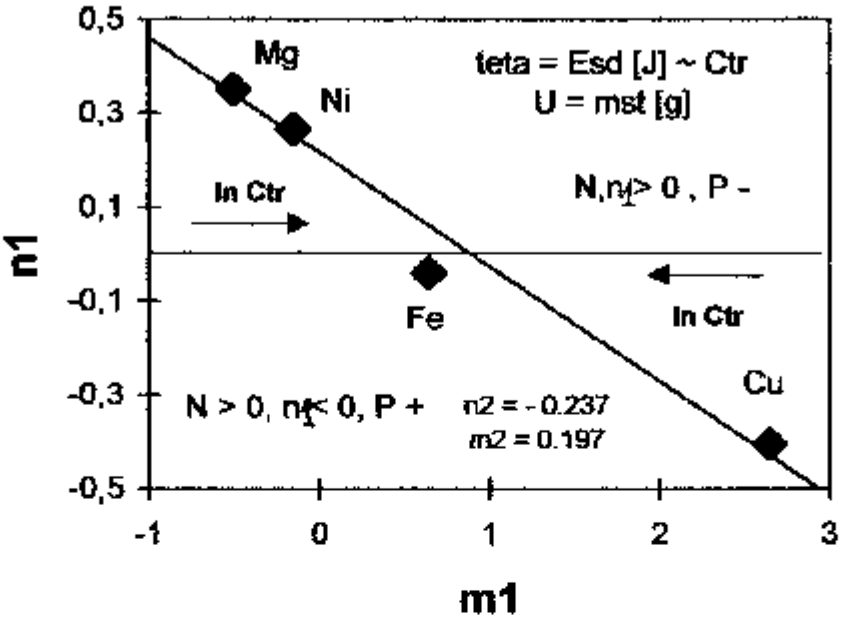

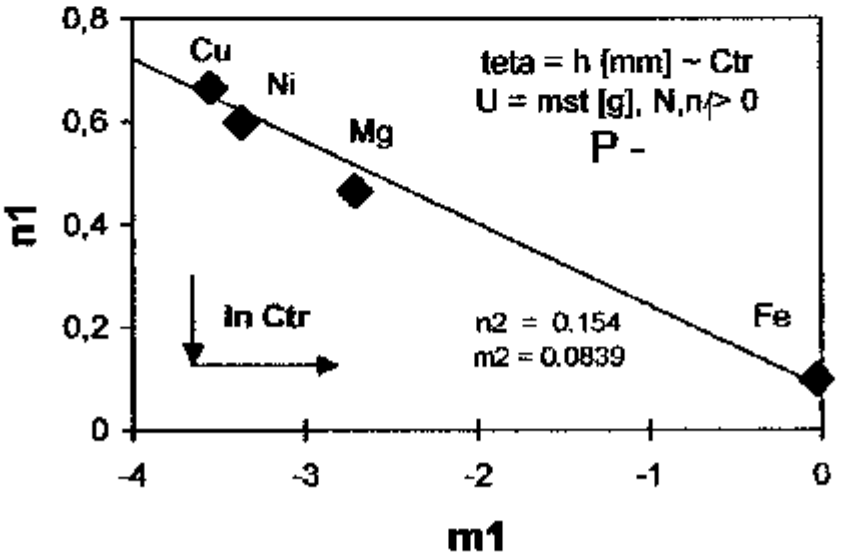

Figure 10. Second philogeny of solution behaviour of several hydrated sulfates as revealed by HRMC according to peak height and overall energy of endotherms as eigenvalues [18].

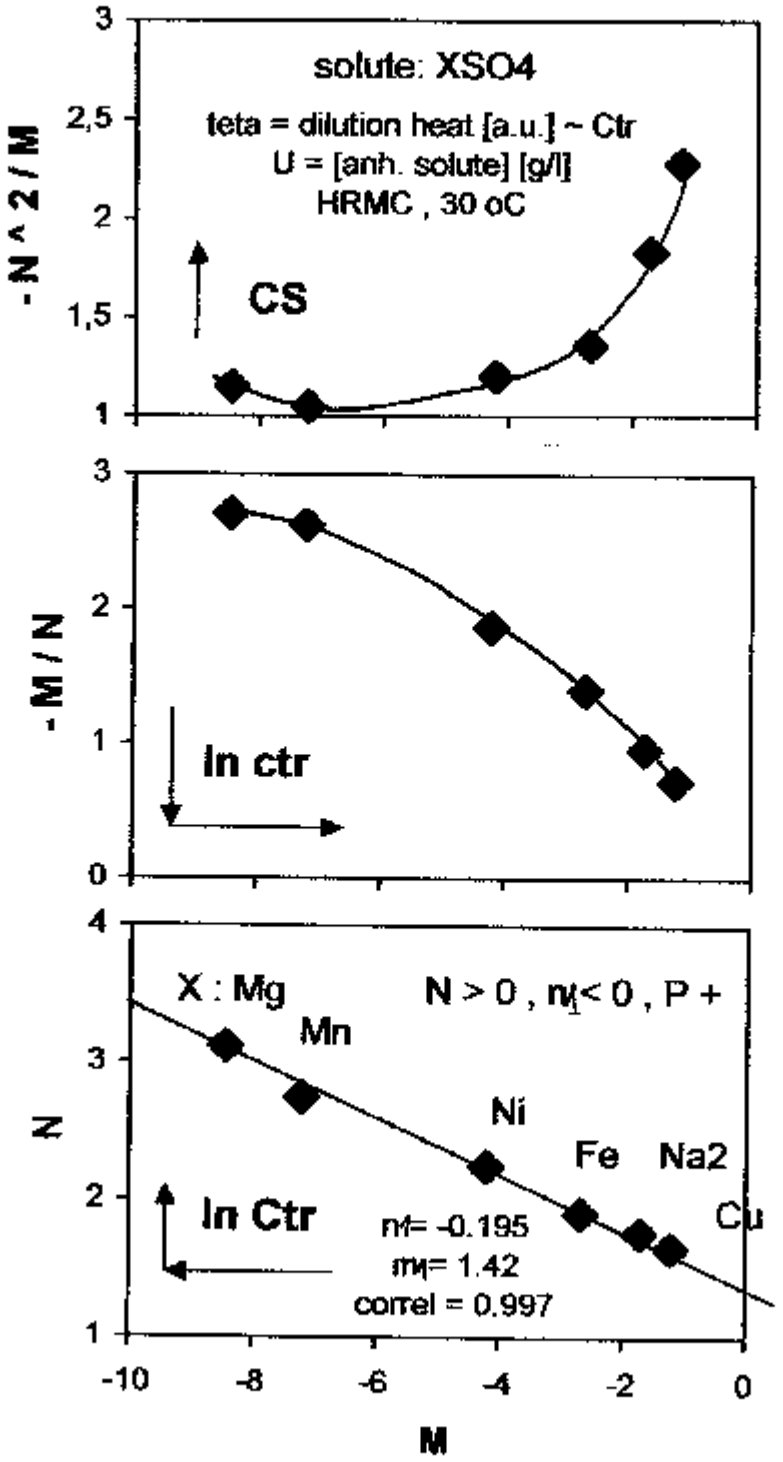

Figure 11. First philogeny of dilution behaviour of several hydrated sulfates as revealed by HRMC [19].

crystallization water has a highly crystalline structure increasing the crystalline fraction of solvent in which the salt hardly penetrates.
Cations have specific potential in making hydrogen bonds in water [18-22]. Figure 9 shows that the solution process has the same nature while the polarity and amplitude drastically changes with crystalline water content for two series of solutes. LiCl has no structuring effect on water. Structuring effect of LiCl and LiBr strongly depends on the crystalline water content, namely: at low content this effect is high (exo) and at maximum content this effect is low or the solubility process changes its polarity (endo) representing the breaking effect of crystalline water. It clearly results that solute penetrates only in the amorphous phase of water up to a specific saturation value depending on other additional potentials as temperature and pressure. Solution process can break more or less the crystalline phase of solvent.
In fact, a solution process consists in contribution of several elementary processes. In general, it coexists structuring and breaking effects in different ratios. These effects were thoroughly studied for a series of several anhydrous and hydrated sulfates by solution and dilution processes [18-23]. Diagrams in Figure 10 show the first phylogenies of solution process for hydrated species of XSO4.nH2O at specific highest crystalline water content by considering two eigenvalues taken from thermograms (all as endothermal) obtained by high resolution mixing calorimetry (HRMC) and mass of solute, mst, as the driving potential [18,20,21]. The peak height of endotherms develops the early stage of solution process which basically represents the breaking effect of crystalline water content in solute, while θ=Esd – the global area of endotherm separates the structuring effect of cations according to the following decreasing order:

$$Cu > Fe > Ni > Mg \qquad (6).$$

This means that for the same amount of anhydrous solute (cst) the caloric effect in solution and dilution experiments has the decreasing order as in relationship (6) reflecting relative value of kinetic entities (ctr) involved in these processes.
Specific contribution of these two contributions may be efficiently revealed by the ratio E/h defining the “caloric pattern” of the tested specimen [33]. The same order of the structuring potential of cations has resulted by dilution process (Figure 11) experienced also by HRMC considering θ=Ed (the global area of dilution thermogram) and U= concentration of solution expressed in (gram of anhydrous salt/ liter of solution) [19]. On the other hand, CS increases with the structuring

potential (Ctr) of cations which is an important practical finding also substantiated by next experimental results.

4. Temperature-pressure-composition behaviour

ACC represents mechanical stresses accumulated in the boundary layers of amorphous and crystalline phases responsible for further behaviour of the overall specimen in a large variety of processing and operating conditions. For this reason, it is important to evidence the nature and the level (amplitude) of these stresses in comparison to CS and the other kinetic (ontogenic and/or phylogenic) parameters as resulted from specific MS.

The general working principle in establishing this relationship is to evidence the sample behaviour in a chosen MS and SOP at different value of externally applied stresses. As topoenergetic behaviour of ACC mainly arises by temperature dependence through the freezing point (by crystallization or melting), the general MS used is called as ***thermomechanical analyzer***. For highly oriented specimens (fibers, yarns) the external stress is applied along the main direction [12]. For almost all studied PE and CPE specimens there is no macroscopic orientation, so the external stress may be applied by isostatic pressure [34].

Further important data on ACC in water and aqueous solutions may be evidenced also by external isostatic pressure as driving potential. Some of simple eigenvalues as a function of temperature, pressure and composition of aqueous solutions are considered in the followings in view to evidence particular aspects of their ACC in the liquid state.

Figure 12 shows the dependences of the main ontogenic parameters as a function of mole fraction of ethanol (EtOH) in aqueous solutions at 25^{o}C for θ= isothermal compressibility =-dV/Vo [d-less] and U= external isostatic pressure = p [Mpa] (experimental data from [35]). Starting to approximately 20 % mole EtOH , EtOH-water clusters progressively increase and Ctr, CS decrease with EtOH content up to saturation values corresponding to pure EtOH. This means that an amorphous-crystalline separation process occurs up to the situation for which EtOH becomes as continuous phase. Isothermal compressibility defines only the behaviour of the amorphous phase, so the threshold value internal stresses in this phase not at ACC of the overall specimen. The dependence po(EtOH) shows two minimum values correspond to plateau shape in the other dependences for the series of aqueous solutions.

Figure 13 shows the dependences of the ontogenic parameters also as a function of [EtOH] for liquid aqueous solutions (at 25 and 50 ^{o}C) for θ=

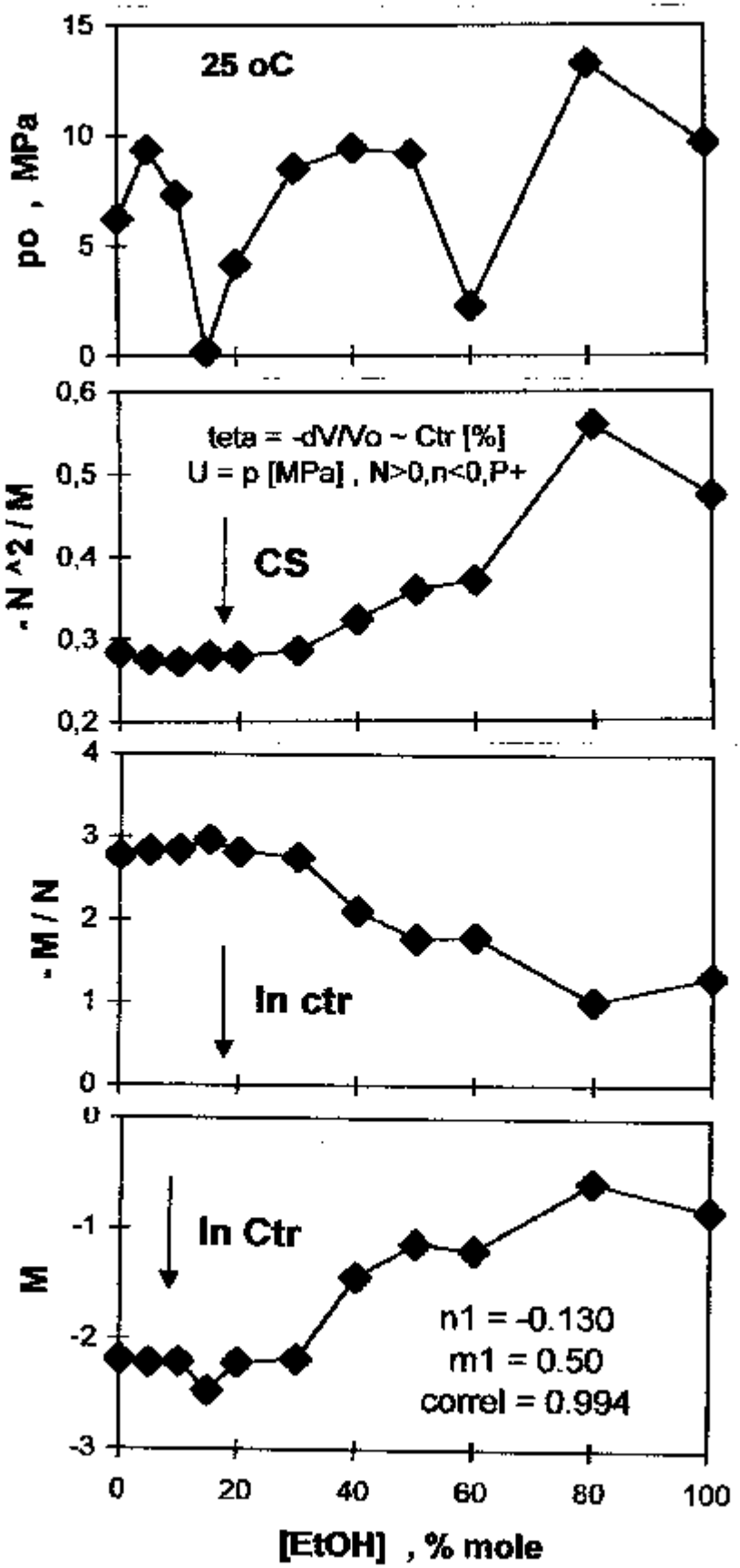

Figure 12. First philogeny of behaviour of aqeuous solutions according to isothermal copressibility as function of [EtOH].

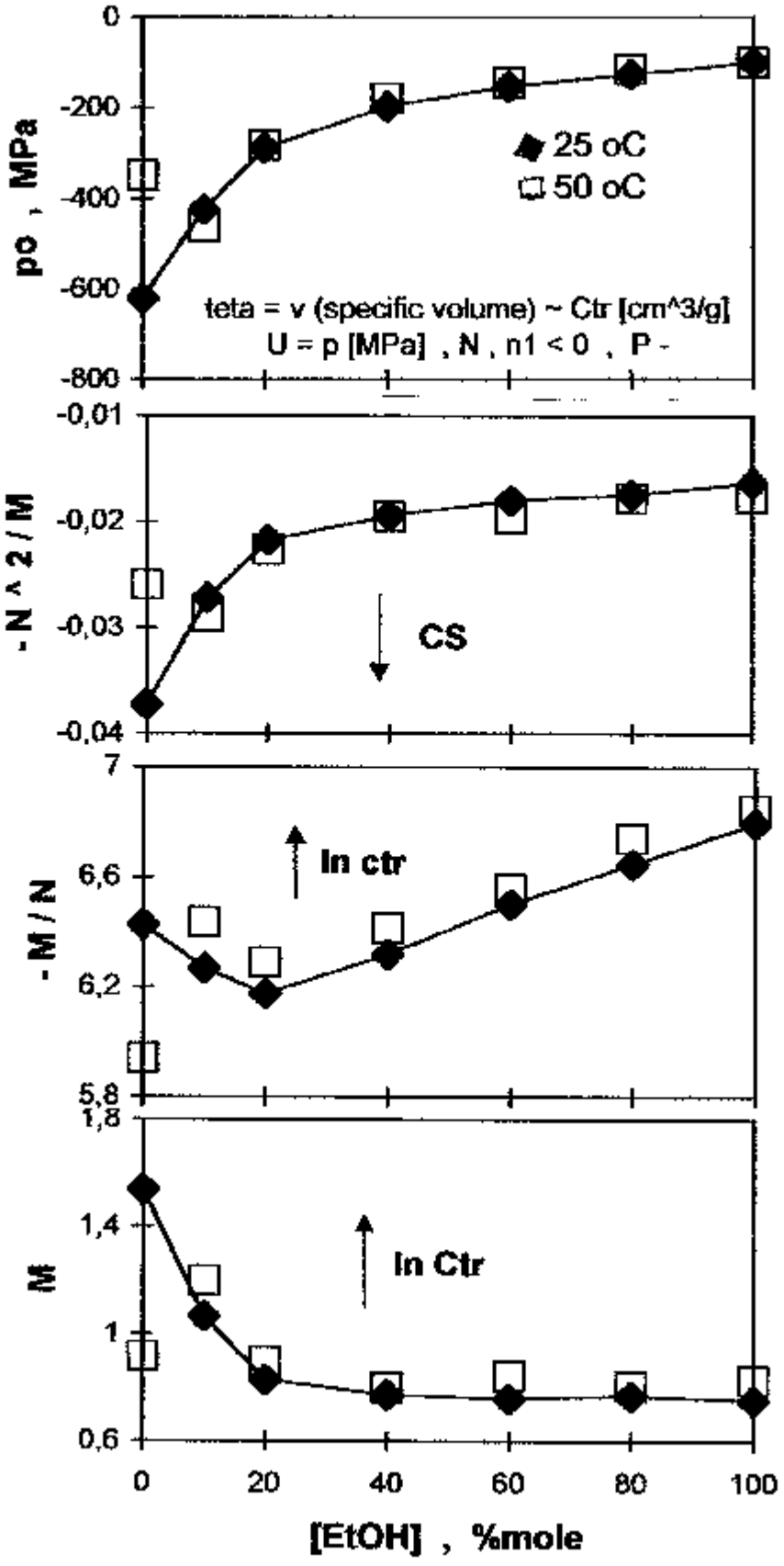

Figure 13. First philogeny of aqueous solutions according to specific volume as function of [EtOH].

specific volume (v) [cm^3/g] and U=p [Mpa] (experimental data from [36]). It is important to notice only the difference in behaviour at pure water between the two considered temperatures , namely at 20 ^{o}C pure water has ACC with maximum value (over 600 Mpa) which progressively decreases with EtOH content. Isothermal compressibility essentially evidences the response of amorphous phase in which the formation of EtOH-water clusters is the main transforming process, while specific volume define the response of the overall specimen for which the transforming process has additional elementary processes. It may observe that Ctr and CS also progressively decrease with EtOH content, but ctr has a maximum value for approximately 20% mole EtOH. This was also observed by kinetic viscosity [35].

Figure 14 shows the dependences of ontogenic parameters as a function of amplitude parameter (M) for a series of water-EtOH solutions at 25 ^{o}C and at different isostatic pressures for θ=water density (do)-solution density (d) [g/cm^3] and U=[EtOH] ,[%mole EtOH] [36].The eigenvalue defines the overall specimen response to addition of EtOH, so Ctr and [EtOH]o increase and ctr and CS decrease with isostatic pressure.These facts are completing the results presented in Figure 13 concerning the behaviour of overall specimens.

Figure 15 shows dependences of ontogenic parameters as a function of isostatic pressure for water-EtOH-KCl solutions and θ=electrical conductance (L) as measured from a specific base line value (Lo) and U=[EtOH] [36]. The results are averaged for [KCl] ranging between (2-8)*10^-4 mole/l and extrapolated to infinite frequency of applied voltage. The electrical conductance essentially defines the response of amorphous phase in which the electrolyte is dispersed. It may observe that Ctr, ctr and Lo decrease and CS increases with the applied pressure. These findings are completing the results presented in Figure 12.

5.Conclusions

The presented results obtained by topoenergetic representation of experimental data on amorphous and overall behaviour of water and aqueous solution in liquid state as a function of temperature, pressure and composition allow to sketch out following main concluding remarks :

1. Morphology of water and aqueous solutions mainly consists in amorphous and crystalline phases periodically distributed each to other (similar to the schematically drawn in Figure 2 for annealed CPE).

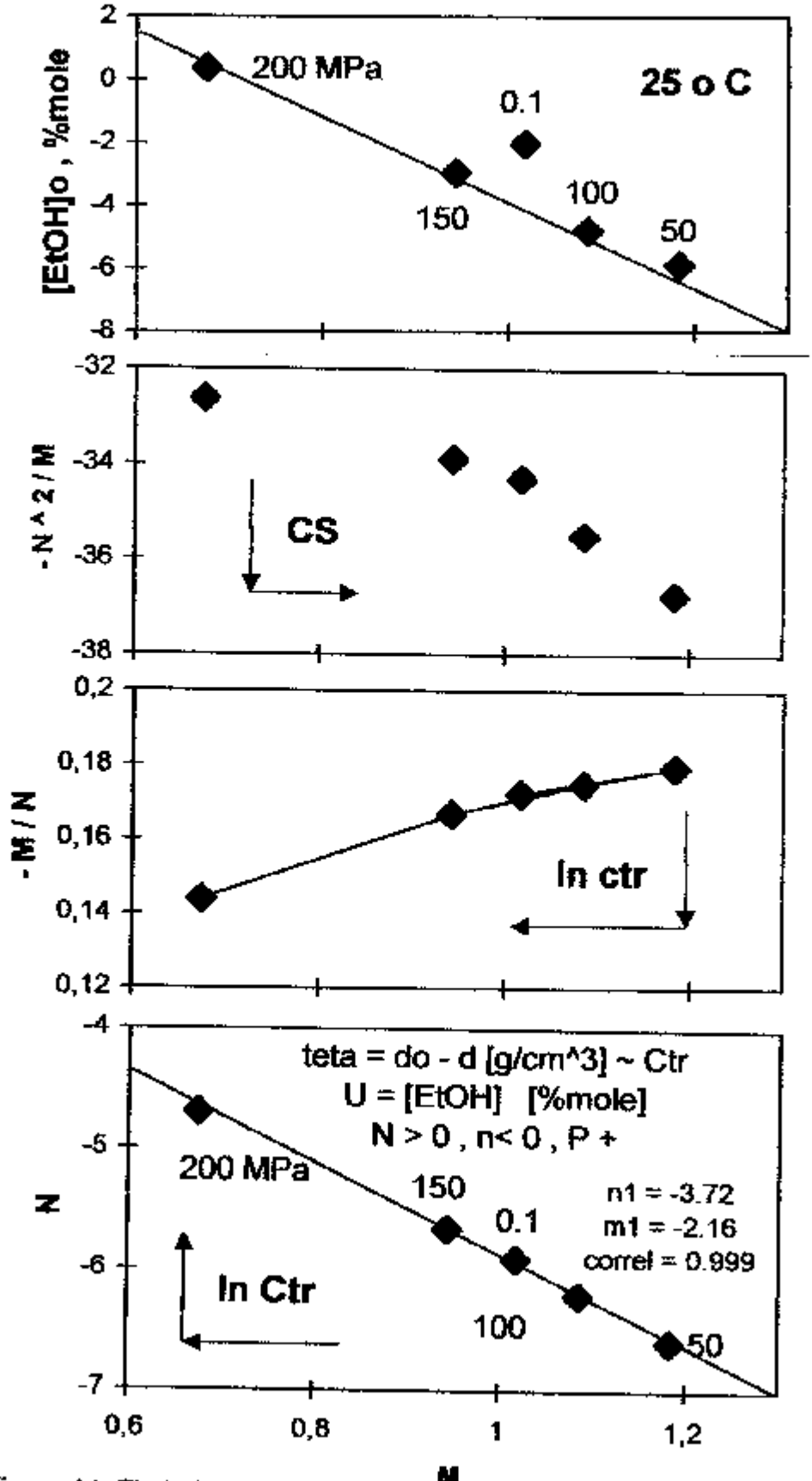

Figure 14. First philogeny of behaviour according to differential density for aqueous solutions.

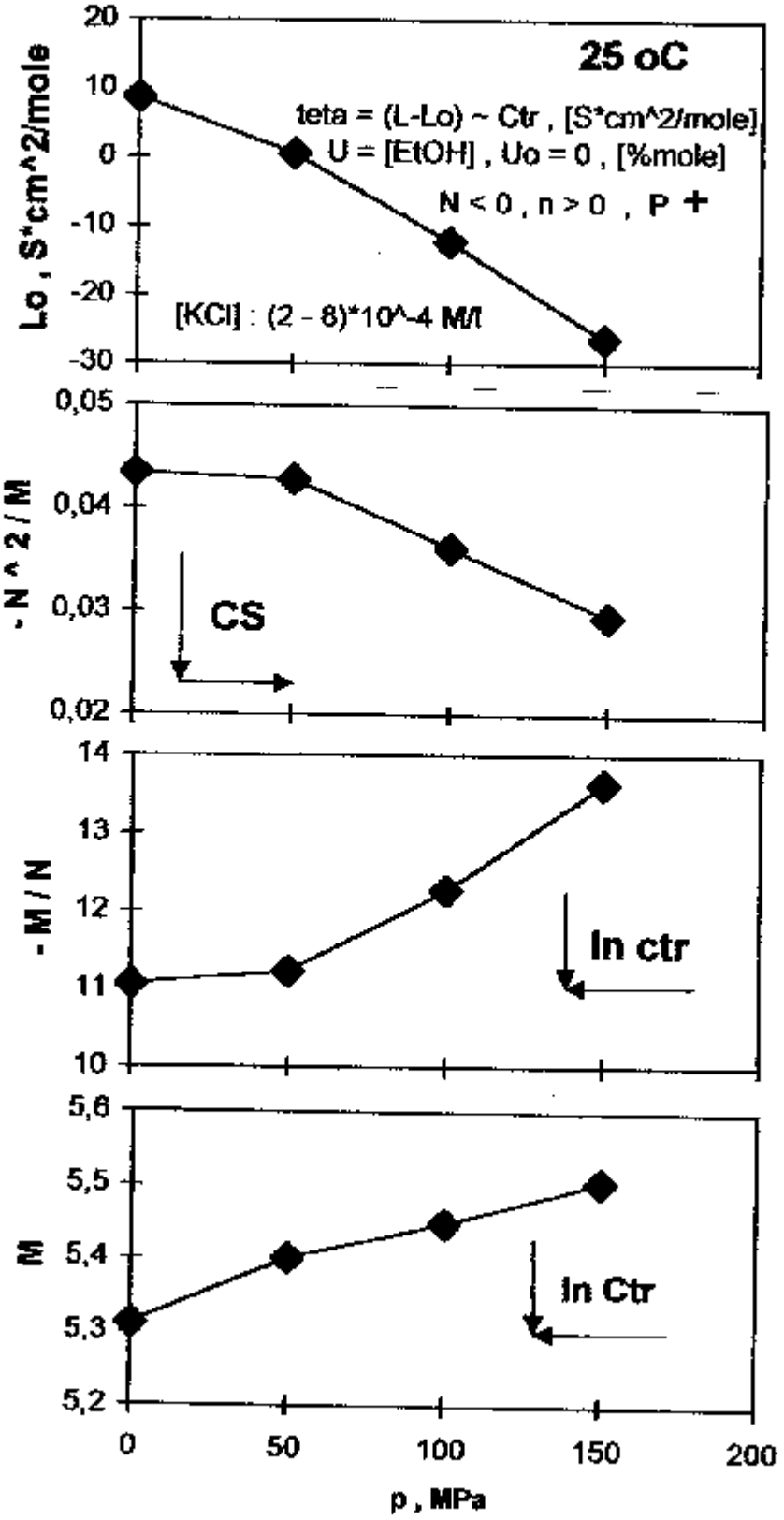

Figure 15. First philogeny of electric conductance of aqueous solutions.

2. ACC of pure water at 20 ^{0}C has highest value (over 600 MPa) in comparison to aqueous solutions. This can explain many particular properties driven by this high potential of water in comparison to other liquids, namely: (i) high superfacial tension; (ii) high capacity and stability in memorizing chemo-thermo-mechanical history (for instance memory of high water dilutions used in homoeopathic practice [24,37]); (iii) nuclear transmutations in the boundary amorphous-crystalline layers in water and other kinds of ACC [15,38,39].
3. Addition of solutes and increase of external pressure decrease ACC in water and aqueous solutions.

References

1. G.Dragan, J.Polymer Sci.,Polymer Symposium,**64**,141-148(1978).
2. G.Dragan,Rev.Roumaine Chim.,**28**(9,10),1315-1326(1981).
3. G.Dragan, Acta Polymerica,**36**(9),499-509(1985).
4. G.Dragan, Rev.Roumaine Chim.,**20**(5),687-698(1975); **21**(9,10),1381-1394(1976).
5. G.Dragan,Materiale Plastice (Bucharest),**10**(2),87-92(1973).
6. G.Dragan,Rev.Roumaine Chim.,**23**(3),435-443(1978).
7. G.Dragan, Acta Polymerica,**37**(10),620-628(1986).
8. G.Dragan, J.Thermal Anal.,**9,**405-414(1976).
9. G.Dragan, Rev.Roumaine Chim.,**21**(9,10),1315-1326(1981).
10. T.Nagasawa and K.Kobayashi ,J.Appl.Phys.,**41**,4276-4282(1970).
11. G.Dragan, Rev.Roumaine Chim,**23**(2),262-264(1978).
12. G.Dragan and C.Oprea, Rev.Roumaine Chim., **30**(6),447-452(1985).
13. G.Dragan, Rev.Roumaine Chim.,**23**(4),629-635 (1978).
14. G.Dragan,Rev.Roumaine Chim.,**21**(11,12)1537-1394(1976).
15. G.Dragan, Fusion Technology ,**20**(3),361-364(1991).
16. C.D.Ellis and W.A.Wooster, Roy.Soc.Proc.**A,117**,109-123(1927).
17. L.Meitner and W.Orthmann,Zeitschrift fur Physik, **60**, 143-155(1930).
18. G.Dragan,J.Thermal Anal.,**31**(3),677-689(1986); **31**(4),941-954(1986).
19. G.Dragan,J.Thermal Anal.,**32**(1),293-300(1987).
20. G.Dragan, Acta Polymerica, **38(**4),211-220(1987).
21. G.Dragan, Acta Polymerica, **38**(5),270-276(1987).
22. G.Dragan, Acta Polymerica, **38**(8),467-470(1987).
23. G.Dragan,Studii si Cercetari de Fizica (Bucharest,english),**43**(7,8),495-508(1991).
24. G.F.Oster and D.M.Auslander, J.Franklin Inst.,**292**,1-21(1971).
25. G.Dragan, Revista de Chimie (Bucarest), **29**(3), 214-217(1978).
26. G.Dragan, Acta Polymerica, **31**(5), 293-298(1980).
27. G.Dragan and F.Stoenescu, Rev.Roumaine Chim**, 24**(1), 55-57(1979).
28. G.Dragan, Acta Polymerica, **37**(11,12),678-684(1986).
29. G.Dragan, J.Thermal Anal., **23**,173-193(1982).
30. G.Dragan, A universal representation of system behaviour based on topoenergetic principles, IXth International CODATA Conference,24-28 June 1984, Jerusalem, Israel (in "The role of data in scientific progress", P.S.Gleaser edt.,North Holland Publ.Co.,1985).
31. G.Dragan,Upon some topoenergetic aspects of DATA BANKS ,12-th International CODATA Conference, Data for discovery, 15-19 July 1990, Columbus, Ohio, USA.

32.M.Broul, J.Nyvlt and O.Sohnel, “Solubility in inorganic two-component systems”,Academy,Prague ,1981.
33.Visco-Dens Calorimeter, VDC-4 , Operating Manual , GDF- DATA BANKS (1996).
34.G.Dragan, Acta Polymerica, **34**(1),1-8(1983).
35.M.Yusa,G.Mathur and R.Stager, J.Chem.Eng.Data, **22**(1),32-35(1977).
36.M.Ueno,N.Tsuchinashi and K.Shimizu, Bull.Chem.Soc.Japan, **58**(10), 2929-2934 (1985); **59**(4),1175-1180(1986).
37.G.Dragan,J.Thermal Anal.,**36**(3),425-431(1992).
38.G.Dragan,Nuclear transmutations in composite systems,The 6^{th} International Conference on Cold Fusion (ICCF-6),13-18 0ctober 1996, Hokkaido, Japan.
39.A clear $D^2 \rightarrow H^1$ process has been observed by annealing of $SnCl_2$ $(H_2O)_x(D_2O)_{2-x}$ single crystals (M.Tatsumi,M.Matsuo,H.Suga and S.Seki, Bull.Chem.Soc.Japan, **52**(3),716-728(1979)).